

## Measurements of the Fluctuation-Induced Flux and the Reynolds Stress in the edge region of ISTTOK

P. Balan,<sup>1</sup> H.F.C. Figueiredo,<sup>2</sup> R.M.O. Galvão<sup>3</sup>, C. Ionita,<sup>1</sup> V. Naulin,<sup>4</sup>  
J.J. Rasmussen,<sup>4</sup> R. Schrittwieser,<sup>1</sup> C.G. Silva,<sup>2</sup> C. Varandas<sup>2</sup>

<sup>1</sup>*Department of Ion Physics, University of Innsbruck, Innsbruck, Austria*

<sup>2</sup>*Centro de Fusão Nuclear – Association EURATOM/IST, Lisboa, Portugal*

<sup>3</sup>*Institute of Physics, University of São Paulo, Brasil*

<sup>4</sup>*Association EURATOM – Risø National Laboratory, Optics and Plasma Research  
Department, Roskilde, Denmark*

### 1. Introduction

Besides edge-localized modes (ELMs) the most important loss mechanism at the edge of magnetically confined toroidal plasmas is the fluctuation-induced particle flux, which may account for a large part of the anomalous energy and particle losses observed. In radial direction the density flux is given by  $\Gamma = \langle \tilde{n}_{pl} \tilde{v}_r \rangle$ , where  $\tilde{n}_{pl}$  are the density fluctuations and  $\tilde{v}_r$  is the fluctuating radial velocity component. Due to ubiquitous low frequency modes (mostly drift wave instabilities) in the edge region there are strong fluctuations of the electric field  $E$  with frequencies well below the ion cyclotron frequency. In this case the fluid velocity can be approximated by the  $E \times B$  velocities, thus the flux becomes:

$$\Gamma = \left\langle \tilde{n}_{pl} \frac{\tilde{E}_\theta}{B_0} \right\rangle, \quad (1)$$

where  $B_0$  is the external toroidal field and  $E_\theta$  is the poloidal component of  $E$ .

A counteracting mechanism might be the Reynolds stress, which is a measure of the anisotropy of turbulent velocity fluctuations and provides the radial flux of poloidal momentum. This produces a stress on the mean flow, which may cause a poloidal flow [1,2,3] if the Reynolds stress has a gradient. The poloidal flow will be sheared, which causes the turbulent eddies to be tilted and elongated in the poloidal direction, thereby reducing the radial turbulent transport [3]. This mechanism plays a key role in explaining the L-H transition and has indeed been found to reduce plasma losses [4]. The Reynolds stress of a turbulent plasma is given by  $R_e = \langle \tilde{v}_r \tilde{v}_\theta \rangle$ , where  $\tilde{v}_\theta$  is the poloidal component of the fluid velocity, i.e.:

$$R_e = \frac{\langle \tilde{E}_\theta \tilde{E}_r \rangle}{B_0^2}. \quad (2)$$

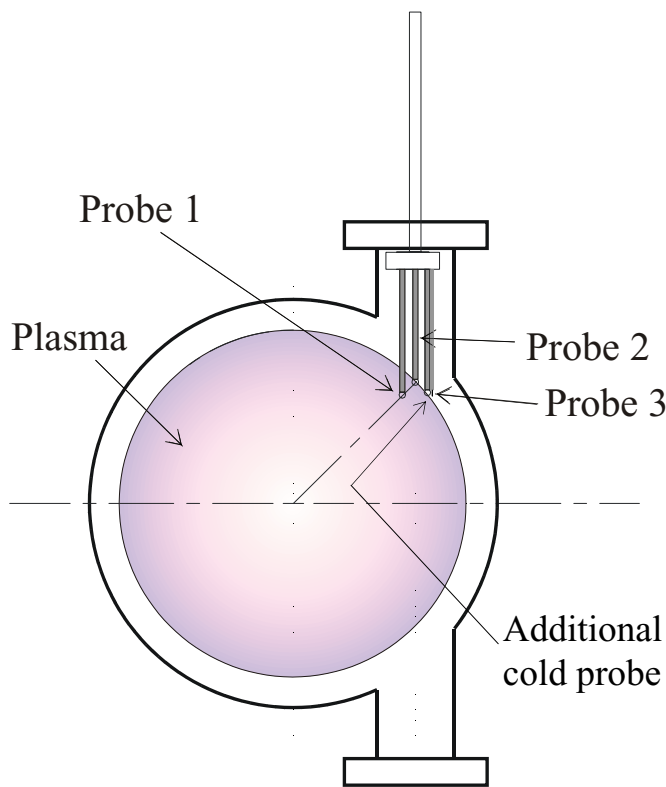


Fig. 1. Schematic of the experimental set-up inserted into a poloidal cross section of ISTTOK.

## 2. Experimental set-up

In an investigation at ISTTOK (Instituto Superior Técnico Tokamak, Lisbon, Portugal; major/minor radius 46 cm and 8.5 cm, respectively; biased limiter at  $r = 7.8$  cm) the Reynolds stress and the fluctuation-induced flux were measured simultaneously. To that end an arrangement of three emissive probes and one cold probe (see Fig. 1) was used in the edge region of the tokamak ISTTOK. The floating potential of emissive probes delivers a better measure for the plasma potential than cold probes since the plasma electron current (and thereby partly

the influence of the electron temperature) is counteracted by the electron emission current [5,6]. With the arrangement shown in Fig. 1, the radial and the poloidal electric field components can be measured at the same time, so that the Reynolds stress  $R_e$  can be derived from the data.

A cold probe is inserted close to one of the outer emissive probes, with which also the fluctuations of the plasma density can be approximated. Therefore, with this arrangement also the radial fluctuation-induced particle flux  $\Gamma$  can be determined.

The general method is to take the floating potentials of the three emissive probes as direct measures of the plasma potentials on a radius and a poloidal meridian. Then the poloidal and radial electric field components  $E_r$  and  $E_\theta$ , respectively, are determined from the formulae  $E_r = (\Phi_{pl,2} - \Phi_{pl,1})/d_{12}$  and  $E_\theta = (\Phi_{pl,3} - \Phi_{pl,2})/d_{23}$  with  $d_{12}$  and  $d_{23}$  being the distances between the respective probes; these are 7 and 5 mm, respectively. The value of  $E_\theta$  was also used for calculating  $\Gamma$ . The fluctuations of the plasma density were determined from those of the ion saturation current  $I_{i,sat}$  to the negatively biased cold probe under the assumption that the fluctuations of the electron and ion temperature  $T_{e,i}$  can be neglected:

$$n_{pl} \cong n_i \cong \frac{1.7 I_{i,sat}}{A_p e} \sqrt{\frac{m_i}{k_B (T_e + T_i)}}, \quad (3)$$

where  $n_i$  is the ion density and  $A_p$  the effective probe area for ion collection.

Since the entire arrangement can be moved radially by a few millimetres, also the radial gradient of  $R_e$ ,  $\partial R_e / \partial r$ , can be determined. However, due to the insertion of the probe arrangement from the side (see Fig. 1) there is an increasing misalignment above and below the most favourable position. In addition, it has to be taken into account, (i) that  $I_{i,sat}$  not only contains density fluctuations but also those of the electron temperature, and (ii) that the method has a limited radial resolution due to the relatively large distances between the emissive probes.

### 3. Results and discussion

Each of the raw signals consists of 8192 points taken with a sampling rate of 500 kHz. It is interesting to note that especially the fluctuations of the poloidal electric field component  $E_\theta$  are strongly negatively skewed.

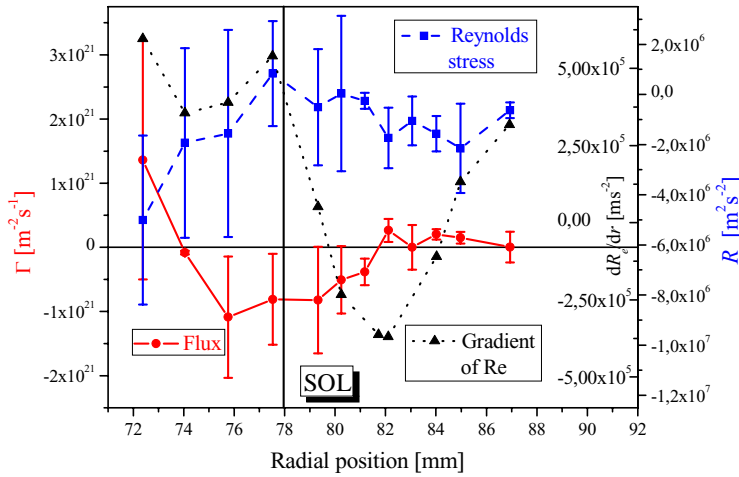


Fig. 2. Preliminary results of the measurements with the probe arrangement: Radial profiles of the radial fluctuation-induced flux  $\Gamma$  (red solid line), of the Reynolds stress  $R_e$  (blue dashed line) and of the gradient of  $R_e$  (black dotted line).

Fig. 2 shows radial profiles of  $\Gamma$  (solid red line) and of  $R_e$  (dashed blue line) in the edge region of ISTTOK, determined on a shot-to-shot basis. Also shown is  $\partial R_e / \partial r$  (black dotted line). The vertical line shows the position of the last closed flux surface (LCFS). The fact that the flux takes negative values, i.e., inward, has to be clarified and

still needs further thorough investigations.

Fig. 3 shows the probability distribution function (PDF) of the Reynolds stress at the radial position of 72 mm, while the shear layer was at 78 mm. The blue curve shows the case when the three probes were unheated so that the probes worked just as cold probes. In this case, the cold probe floating potentials  $V_{fl}$  were used as approximations for the plasma potentials. The red curve has been obtained with the probes heated to electron emission so

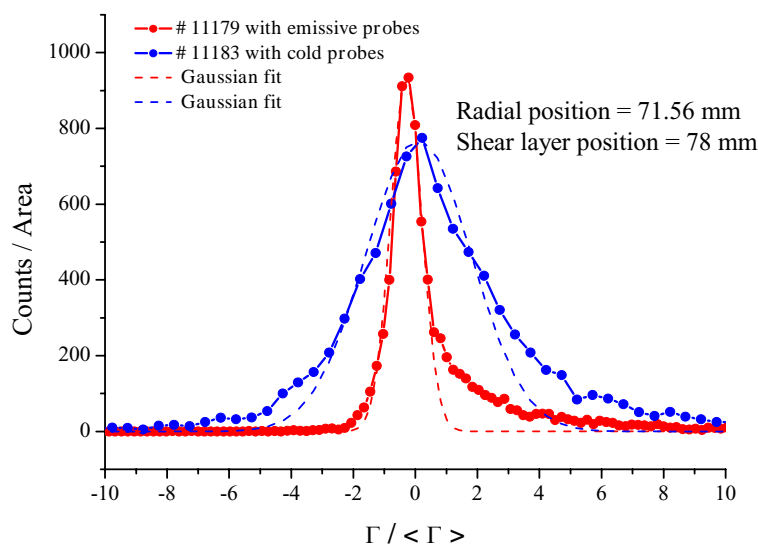


Fig. 3. Probability distribution function (PDF) of  $R_e$  at  $r \approx 72$  mm, once determined by the three probes unheated (blue) and once heated (red). The blue and red dotted lines show the corresponding fitted Gaussians.

shown by blue and red dashed lines in the figure. An asymmetric PDF is also a sign for a radial momentum flux and therefore for the generation of poloidal flows.

These results are preliminary and the errors induced by the misalignment of the probes in the poloidal/radial direction on the evaluation of the fluctuation-induced flux will be further investigated. Nevertheless, we are convinced that our results show the correct trend: the flux is suppressed in regions of sheared poloidal flows.

We have shown that in principle with our arrangement of three emissive probes and one cold probe the Reynolds stress  $R_e$  and the fluctuation-induced flux  $\Gamma$  can be measured simultaneously in the edge region of a small tokamak. In previous investigations the Reynolds stress has only been measured with cold probes, and no simultaneous measurements of the flux have been presented [2].

Acknowledgements: This work has been carried out within the Association EURATOM-IPP and EURATOM-ÖAW. The content of the publication is the sole responsibility of its author(s) and it does not necessarily represent the views of the Commission or its services. The support by the Fonds zur Förderung der wissenschaftlichen Forschung (Austria) under grant No. P-14545 is acknowledged.

## References

- [1] P.H. Diamond and Y.B. Kim, *Phys. Fluids B* 3 (1991), 1626.
- [2] C. Hidalgo et al., *Phys. Rev. Lett.* 83, 2203 (1999).
- [3] S.B. Korsholm et al., *Plasma Phys. Control. Fusion* 43, 1377 (2001).
- [4] K.H. Burrell, *Phys. Plasmas* 4 (1997), 1499; P.W. Terry, *Rev. Mod. Phys.* 72 (2000), 109.
- [5] R. Schrittwieser et al., *Plasma Phys. Contr. Fusion* 44 (2002), 567.
- [6] P. Balan et al., *Rev. Sci. Instrum.* 74 (2003), 1583.

that a better approximation of the plasma potential was used as a basis for calculating  $R_e$ , with the influence of  $T_e$ -fluctuations minimized. The PDF determined with the emissive probes is narrower but it also shows a more non-Gaussian character than that determined with the cold probes. This can be seen by comparison with the respective Gaussian PDFs that are also